Letter

Stable infinite-temperature eigenstates in SU(2)-symmetric nonintegrable models

Christopher J. Turner,[1] Marcin Szyniszewski,[1,2,*] Bhaskar Mukherjee,[1,3] Ronald Melendrez,[4,5] Hitesh J. Changlani,[4,5] and Arijeet Pal[1]

[1]*Department of Physics and Astronomy, University College London, Gower Street, London WC1E 6BT, United Kingdom*
[2]*Department of Computer Science, University of Oxford, Parks Road, Oxford OX1 3QD, United Kingdom*
[3]*S. N. Bose National Centre for Basic Sciences, Block JD, Sector III, Salt Lake, Kolkata 700106, India*
[4]*Department of Physics, Florida State University, Tallahassee, Florida 32306, USA*
[5]*National High Magnetic Field Laboratory, Tallahassee, Florida 32310, USA*

(Received 11 October 2024; accepted 29 April 2026; published 30 June 2026)

Nonintegrable many-body quantum systems typically thermalize at long times through the mechanism of quantum chaos. However, some exceptional systems, such as those harboring quantum scars, break thermalization, serving as testbeds for foundational problems of quantum statistical physics. Here, we investigate a class of nonintegrable bond-staggered models that is endowed with a large number of zero-energy eigenstates and possesses a non-Abelian internal symmetry. We use character theory to give a lower bound on the zero-energy degeneracy, which matches exact diagonalization results and is found to grow exponentially with the system size. We also show that few-magnon zero-energy states have an exact analytical description, allowing us to build a basis of low-entangled fixed-separation states, which is stable to most perturbations found in experiments. This remarkable dynamical stability of special states elucidates our understanding of nonequilibrium processes in non-Abelian chaotic quantum models.

DOI: 10.1103/rsm1-hzc3

Introduction. The concept of nonintegrability is closely associated with the thermalization of all eigenstates of a many-body quantum system, alongside their complex chaotic behavior [1–4]. At long times, the average properties of such systems can be described using the microcanonical ensemble of statistical mechanics, effectively erasing all information about initial conditions to local observables [1,5,6]. Despite this statistical description, nonintegrable models remain analytically intractable [7–9]: Unlike integrable systems, they lack an extensive set of local integrals of motion (see the methodology of Ref. [10] and its subsequent applications [11–13]), leaving numerical treatments our primary source of understanding.

However, certain nonintegrable models have recently been found to defy such a statistical description. Examples include systems with many-body quantum scars [14–22], which are atypical states within the spectrum that violate the eigenstate thermalization hypothesis and sometimes can be constructed exactly. Often these are characterized by low entanglement, but sometimes occur with volume-law entanglement [23–26]. These out-of-equilibrium states are gaining interest as their anomalous dynamics may provide useful resources for state preparation, dynamical control, and quantum simulation on programmable quantum platforms [27–30].

*Contact author: mszynisz@gmail.com

Interestingly, the existence of degenerate manifolds can also signify potential analytical tractability, with applications spanning low-energy physics [31], the order by disorder mechanism in frustrated magnetism [32–35], and fault-tolerant quantum computation [36–38]. Specifically, zero-energy degeneracy (ZED) plays a crucial role in topological phases [37,39,40], where it informs about the dimension of the ground-state manifold, thereby revealing the quantum information capacity of the topologically protected state. Typically arising due to symmetry, zero-energy eigenstates have been recently studied in the celebrated PXP model in the context of thermalization [17]. These PXP zero-energy states exhibit several interesting properties, including area-law entanglement [18], stability in experimental setups [41], and being building blocks for quasiparticle excitations [18,42]. Furthermore, certain lattice gauge theory models are endowed with constructible zero-energy many-body quantum scars [43–45].

This raises questions about whether zero-energy subspaces in other models [46] might demonstrate analogous fascinating characteristics. Of particular interest would be an exploration of models with complex internal symmetries that have not been studied before. In this Letter, we investigate a class of nonintegrable bond-staggered (alternating) spin chains that possesses a non-Abelian internal symmetry. These models have attracted both theoretical [47–49] and experimental [50,51] interest due to their connection to Haldane spin chains and resemblance to the Su-Schrieffer-Heeger model. Here, we employ character theory to obtain null-space degeneracies within each symmetry sector, which we find to be scaling exponentially with the system size. Through symmetry considerations, we are able to construct a nontrivial exact zero-energy basis, serving as a few-body scarred subspace.

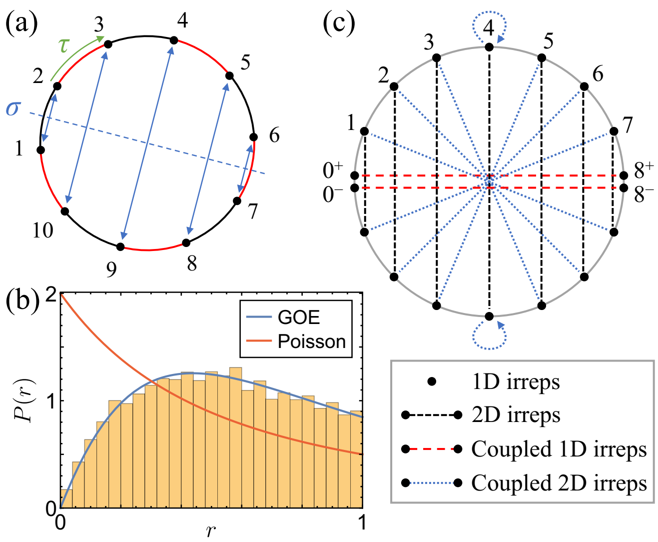

FIG. 1. (a) Spatial symmetries of the bond-staggered Heisenberg chain of size $L = 10$: reflection symmetry σ (blue) and translation τ (green). (b) Level statistics for $L = 22$, $S = 0$, $S^z_{\text{tot}} = 0$, showing a chaotic behavior of the ratio of consecutive level spacings r (Gaussian orthogonal ensemble distribution). Integrable models follow the Poisson distribution. To improve the statistics, the results are gathered for all constant momenta sectors $0 < k < \pi$. (c) Representation theory of D_{2L} for $L = 16$. Each representation labeled by integer momentum κ is coupled by the antisymmetry group $\mathcal{A}$ (red and blue lines).

This fixed-separation basis possesses low entanglement and is remarkably stable to experimental perturbations. These results push our current understanding of the dynamical stability of special states in non-Abelian chaotic models.

Model. Consider a class of bond-staggered Heisenberg spin chains defined on a periodic lattice of L sites,

$$H = \sum_{i=1}^{L} (-1)^i \, \mathbf{S}_i \cdot \mathbf{S}_{i+1} + V \tag{1a}$$

$$= \frac{1}{2} \sum_i (-1)^i \, \text{SWAP}_{(i,i+1)} + V, \tag{1b}$$

where $\mathbf{S}_i = (S^x_i, S^y_i, S^z_i)$ is the vector of spin-half operators and V is any perturbation that preserves the symmetries of the model, as defined below. The presence of the perturbation term makes our results generic while allowing for investigations of stability against external disruptions. The second equality allows us to interpret the Hamiltonian as a collection of SWAP gates, which will prove useful in subsequent analysis. The model is endowed with a non-Abelian SU(2) total spin symmetry and the total spin conservation in any direction [U(1) symmetry]; without a loss of generality, we consider conservation of $S^z_{\text{tot}} = \sum_i S^z_i$. This forms the internal symmetry group $\mathcal{G}$. The Hamiltonian (1a) anticommutes with the translation operator τ and commutes with translation by two sites, τ^2, and with bond-reflection symmetry, σ. Together, these form the spatial symmetry group of the model, the dihedral group D_L, illustrated in Fig. 1(a). We term the D_{2L} group generated by τ and σ the antisymmetry group $\mathcal{A}$.

Previous research [52,53] has implied that staggering the interaction term is responsible for breaking the integrability of the Heisenberg chain. We show this explicitly through level statistics for the periodic model with $V = 0$ by resolving all its symmetries. We write the Hamiltonian in the fixed momentum magnon basis [54], which resolves S^z_{tot} and τ^2. $\mathbf{S}^2$ is resolved by comparing the spectra of two consecutive values of S^z_{tot}, while σ is diagonalized directly. We then plot the distribution of the ratio of consecutive level spacings r [55] in Fig. 1(b), which we find to match the prediction for the Gaussian orthogonal ensemble (GOE) of random matrix theory [56]. This implies the model is chaotic, strongly suggesting its nonintegrability. Moreover, the distribution exhibits level repulsion at $r = 0$, while if the model had some remaining symmetries or was integrable, repulsion would be absent and the histogram would resemble the Poisson distribution.

Zero-energy states enforced by the symmetry. Through symmetry considerations, we calculate the lower bound on the null-space dimension of the Hamiltonian and compare the result with exact diagonalization. The intuition for why the symmetry can inform about ZED is as follows. Consider any Hamiltonian H that anticommutes with some unitary operator A, thus implying a symmetric spectrum ($E \mapsto -E$). Suppose that A has only real eigenvalues, ± 1, with multiplicities m_+ and m_-. In the eigenbasis of A, the Hamiltonian takes a block off-diagonal form, consisting of blocks of sizes ($m_+ \times m_-$). Consequently, $H^2 = H^\dagger H$ becomes block diagonal, separating into two sectors of A, with dimensions ($m_+ \times m_+$) and ($m_- \times m_-$), both necessarily of the same rank. If there is an imbalance between m_+ and m_-, then the null space of H^2 (and consequently the null space of H) is at least $|m_+ - m_-|$ dimensional [57]. Note that ZED may be larger if both sectors contain zero-energy states. However, if the model is chaotic, the lower bound is expected to be saturated.

This idea is refined when the anticommuting operator is part of a larger antisymmetry group. We find that the $\mathcal{A}$ sectors are paired by the action of H as (1) one-dimensional irreducible representations labeled by momenta $k = 0$ and $k = \pi$ with the same reflection eigenvalue $s = \pm 1$ and (2) the two-dimensional irreps with momenta k and $(\pi - k)$, with $k = 2\pi\kappa/L$, where $\kappa = 1, \ldots, L/2 - 1$ [see Fig. 1(c)]. Hence, ZED is bounded by

$$\mathcal{Z} \geqslant \sum_{s=\pm 1} |m_{0,s} - m_{L/2,s}| + 2 \sum_{\kappa=1}^{\lfloor (L-2)/4 \rfloor} |m_\kappa - m_{L/2-\kappa}|, \tag{2}$$

where $m_{\kappa,s}$ are the multiplicities of the antisymmetry representation labeled by (κ, s), with the s label suppressed in the second sum as it is forced by κ. This is enhanced by internal symmetries, which cause the computation to be performed in each $\mathcal{G}$ sector separately.

We can calculate these symmetry-resolved multiplicities using character theory [58,59]. The character function $\chi_\rho(g) = \text{tr}(\rho(g))$ is a function that identifies a representation ρ. Specifically, we take the character function for the representation on the full Hilbert space $\mathcal{H}$ and we use the Schur orthogonality relations for the natural inner product: The multiplicity of each irreducible representation within that full representation is the inner product of the irrep character and the character of the full representation. Due to the product

TABLE I. Zero-energy degeneracy $\mathcal{Z}$ of the bond-staggered Heisenberg model as a function of total spin quantum number S and system size L, from numerics. The numbers in parentheses are from the character theory (absent if theory matches numerics). Extra zero-energy states are highlighted in bold font.

L	$S=0$	1	2	3	4	5	6	7	8	9	10	11	Total
4	0	1	1										8
6	3	3	1	1									24
8	0	**6 (2)**	2	1	1								**44 (32)**
10	10	10	7	7	1	1							144
12	**2 (0)**	7	7	4	4	1	1						**146 (144)**
14	**37 (35)**	35	27	27	11	11	1	1					**714 (712)**
16	**4 (0)**	14	14	14	14	6	6	1	1				**516 (512)**
18	126	126	102	102	52	52	15	15	1	1			3224
20	0	50	50	48	48	31	31	8	8	1	1		2208
22	462	462	390	390	225	225	85	85	19	19	1	1	14136

structure of the group we are interested in, we can write this full character as a function of $g \in \mathcal{A}$ and $\theta \in \mathcal{G}$. This allows the inner product to be taken in two steps, first over the spatial part to produce $F_{\kappa,s}(\theta) = \langle \chi^{\mathcal{A}}_{\kappa,s}(g), \chi_{\mathcal{H}}(g,\theta)\rangle_{\mathcal{A}}$. Note that $\chi^{\mathcal{A}}_{\kappa,s}(\sigma^\nu \tau^\mu) = d_\kappa s^\nu \cos(2\pi\kappa\mu/L)$, where $d_\kappa \in \{1,2\}$ is the dimensionality of irrep κ (see the Supplemental Material [60]). Second, over the internal symmetry group to extract the multiplicity of an individual representation,

$$m_{\kappa,s,S} = \langle \chi_S(\theta), F_{\kappa,s}(\theta)\rangle_{\mathcal{G}}, \tag{3}$$

where S labels the total spin sector. Note that one does not need to resolve S^z_{tot}, as it only acts inside each SU(2) representation.

Now, viewing g as a permutation of sites, we can use its decomposition into cycles of sites,

$$\chi_{\mathcal{H}}(g,\theta) = \mathrm{tr}_{\mathcal{H}} g\theta = \prod_{\gamma \in \text{cycles of } g} \mathrm{tr}_\gamma(\tau\theta) = \prod_l \left[\mathrm{tr}_{\mathcal{H}_l}(\tau\theta)\right]^{c_l(g)}, \tag{4}$$

where $c_l(g)$ is the l-cycle index of g that counts the number of cycles of length l in g, see Supplemental Material [60]. The final trace appearing in Eq. (4) is over a system of size l (Hilbert space $\mathcal{H}_l$) and we call this the l-cycle character function. Analogously to its use for the single-site translation, we use τ here to refer to the generator of the cyclic group within each cycle.

At this point, we specialize to the main internal symmetry of interest, SU(2). The character function for the irreducible representation of spin S is $\chi^{\mathrm{SU(2)}}_S(\theta) = \sin[(2S+1)\theta]/\sin\theta$ [58], and this forms a basis for the space of character functions. Pointwise operations on these produce a ring, known variously as the character ring or representation ring, and are equivalent to the fusion rules of SU(2) [61]. This equivalence takes the tensor product of representations to pointwise multiplication of characters and direct sum to addition, producing equations such as $\chi^{\mathrm{SU(2)}}_{1/2}\chi^{\mathrm{SU(2)}}_{1/2} = \chi^{\mathrm{SU(2)}}_0 + \chi^{\mathrm{SU(2)}}_1$ from the fusion rules of SU(2). The character function for the l cycle evaluates to

$$\mathrm{tr}_{\mathcal{H}_l}(\tau\theta) = 2\cos l\theta = \chi^{\mathrm{SU(2)}}_{l/2}(\theta) - \chi^{\mathrm{SU(2)}}_{l/2-1}(\theta). \tag{5}$$

Finally, we perform polynomial-complexity arithmetic in this ring, see Supplemental Material [60], and combine Eqs. (2)–(5) to compute the zero-energy degeneracies in any sector.

We compare the number of zero-energy eigenstates predicted by the character theory with the exact diagonalization results for $V = 0$ in Table I and find an almost exact match, except for a few extra zero-energy states for small system sizes, see Supplemental Material [60]. This additional degeneracy is most likely accidental, occurring due to small symmetry sector size, rather than from an unresolved symmetry, for which we see no evidence. The degeneracy can be lifted with the addition of a perturbation, such as $V = \lambda \sum_i (-1)^i \mathbf{S}_i \cdot \mathbf{S}_{i+3}$ for a generic perturbation strength λ, while respecting the symmetries. Another interesting finding is a correspondence between multiplicities in sectors $\{S = L/2 - 2n, k, s\}$ and $\{S-1, \pi - k, -s\}$, which we observe in character theory results across all available system sizes (up to $L = 42$). We note, however, that this correspondence is a mathematical property coming from the arithmetic of the cycles in Eq. (5), and does not imply the existence of a simple operator that maps states between the two sectors.

We observe that the ZED grows exponentially with a rate half that of the state space dimension, $\ln\mathcal{Z} \sim \ln(2^{L/2})$ (see Fig. 2). Interestingly, a similar system size dependence has been seen previously in the PXP model [17]. The significant fraction of zero-energy states comes from the $k = 0$ and $k = \pi$ sectors (the one-dimensional representations), which can be shown to follow $\mathcal{Z} \geqslant 2^{L/2+1}$, see Supplemental Material [60]. This simple prediction works especially well when L is a power of 2, for in that case the character-theoretic zeros are only found in these sectors. Similarly, as seen in the inset of Fig. 2, for $L = 4n$, there are relatively few additional zeros, while for $L = 4n + 2$, other sectors contribute substantially more.

Exact zero-energy basis. This exponentially large null space predicted by the character theory motivates our search for special analytically tractable states. Remarkably, we find that certain zero-energy states can be expressed in a closed form. In the following, we demonstrate how to construct a basis for two-magnon states, where the constant number of magnonic excitations is $N_{\mathrm{mag}} = L/2 - S^z_{\mathrm{tot}}$. The case of zero and one magnons is trivial, as there exists up to one zero-energy state per symmetry sector.

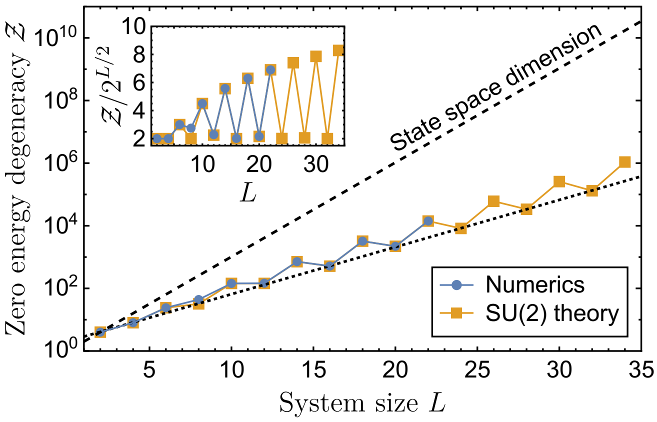

FIG. 2. Zero-energy degeneracy $\mathcal{Z}$ as a function of the system size for the numerical results and character theory. The dashed line is the state space dimension of 2^L, while the dotted line shows $2^{L/2+1}$. The inset shows $\mathcal{Z}/2^{L/2}$.

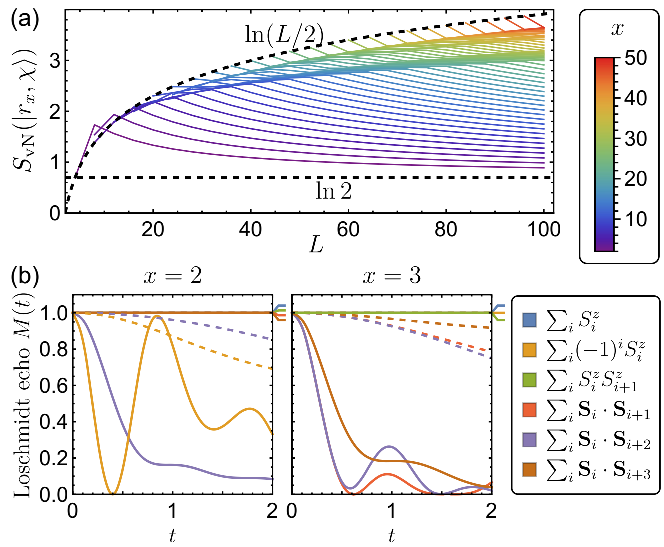

FIG. 3. (a) Entanglement entropy S_{vN} for the states of constant separation $|r_x;\chi\rangle$. (b) Loschmidt echo $M(t)$ for chain of size $L=32$, with magnon separations $x=2$ (left) and $x=3$ (right). The strength of perturbation terms is $\lambda=0.1$ (dashed lines) and $\lambda=1.0$ (solid lines).

We use the computational basis with defined magnon positions and assume the system size is divisible by 4. Using the action of $\mathcal{A}$, we partition this basis into orbits, $\mathrm{Orb}_{\mathcal{A}}(r_x)=\{g\,|r_x\rangle : \forall\, g\in\mathcal{A}\}$. Each orbit comes from a representative element $|r_x\rangle$, where the magnons have a defined separation $x\geqslant 1$, which uniquely identifies an orbit. Then within an orbit, we can produce a basis for the one-dimensional representations with character theory, creating symmetrized states

$$|r_x;\chi\rangle=\frac{\sqrt{|\mathrm{Orb}_{\mathcal{A}}(r_x)|}}{|\mathcal{A}|}\sum_{g\in\mathcal{A}}\chi(g)\,g|r_x\rangle\,. \tag{6}$$

Each orbit contains a so-called 0 representation denoted by χ_0, which sets $\chi(\tau)=+1$ and gives an orbit-dependent sign for $\chi(\sigma)$. Every orbit, except for the orbit with separation $L/2$, has a so-called π representation denoted χ_π, which sets $\chi(\tau)=-1$ and again gives an orbit-dependent sign for $\chi(\sigma)$. The reflection-parity signs are irrelevant for the fixed-separation states, justifying suppressing them from the notation.

Consider the action of H in the form of Eq. (1b) with $V=0$ upon some representative element $|r_{2n}\rangle$ with even separation, where $n=1,\ldots,L/4$. Applying a SWAP that is not incident on either magnon leaves the representative invariant, because there are just as many such positive and negative SWAPS. Hence, $\langle r_{2n};\chi_0|\,H\,|r_{2n}\rangle=0$. If we use a SWAP to move one of the magnons to the left, we increase the separation, and for the other magnon, this happens if we SWAP it to the right. Because their initial separation is even, these SWAPS have opposite signs; hence, $\langle r_{2n+1};\chi_0|\,H\,|r_{2n}\rangle=0$, since the contributions will destructively interfere. A similar argument can be used to show that odd separation representatives satisfy $\langle r_{2n+1};\chi_\pi|\,H\,|r_{2n+1}\rangle=0$ and $\langle r_{2n+2};\chi_\pi|\,H\,|r_{2n+1}\rangle=0$. Combining these results, we obtain

$$H\,|r_{2n};\chi_\pi\rangle=0 \quad \text{for } n=1,\ldots,L/4, \tag{7a}$$

$$H\,|r_{2n+1};\chi_0\rangle=0 \quad \text{for } n=1,\ldots,\lfloor(L-2)/4\rfloor. \tag{7b}$$

Since the orbits are disjoint, this describes $(L/2-1)$ mutually orthogonal zero-energy eigenstates. The final zero-energy state comes from the uniform superposition in the computational basis, which is part of the maximum spin multiplet. In conclusion, when L is a multiple of 4, we can construct an exact basis for all $L/2$ zero-energy eigenstates in the one-dimensional irreps of $\mathcal{A}$.

Entanglement and stability of the fixed-separation basis. Given their analytical tractability, we inquire whether these zero-energy states are endowed with interesting physical properties, such as being interacting quantum scars. We discover that the states with fixed magnon separation exhibit an area-law von Neumann entanglement entropy scaling [see Fig. 3(a)], see Supplemental Material [60], whose value approaches $\ln 2$ in the infinite-volume limit. Conversely, if the separation scales linearly with the system size, the entropy behaves as expected for a generic state in a two-magnon sector, i.e., $\sim\ln L$.

Surprisingly, the proposed basis is exceptionally stable to external perturbations. Consider the following terms that may naturally arise in experimental setups [62–66]: external field, staggered field, Ising interaction, and extended Heisenberg interaction. We assess the stability of each state by measuring the Loschmidt echo at time t,

$$M(t)=|\langle\psi|e^{i(H_0+\lambda V)t}e^{-i(H_0-\lambda V)t}|\psi\rangle|^2, \tag{8}$$

where V is the perturbation in question and λ is its strength. We use representative examples of even/odd separation states to be those of $x=2$ and $x=3$, respectively. In each class, the qualitative behavior is the same. As shown in Fig. 3(b), we find that the basis is remarkably stable: States of even separations are only unstable to the staggered field and $\sum_i \mathbf{S}_i\cdot\mathbf{S}_{i+2}$, while odd-separation states are unstable to Heisenberg-type interaction terms. This implies that one can form a stable fixed-separation basis of zero-energy states, which can be used to encode some initial quantum information. This information is then preserved for a long period of time if the strength of the destabilizing perturbations is small.

Interestingly, the Loschmidt echo for the staggered field perturbation shows an unusually strong revival at $t \approx 1$, $\lambda = 1.0$, implying that one can recover the initial state even if the additional term generally destroys the coherence of the state.

Discussion. In this Letter, we have investigated a class of bond-staggered Heisenberg models. Despite their relative simplicity as two-body Hamiltonians, they exhibit rich physics, including a large number of zero-energy states. Through symmetry considerations, we provided the lower bound on the zero-energy degeneracy, showing that the null space grows exponentially with the system size. Furthermore, we constructed exact analytical formulas for up to two-magnon solutions using character theory. This fixed-separation zero-energy basis exhibits low entanglement and remarkable stability when subjected to perturbations that naturally occur in experiments.

This research opens up several exciting future directions. First, can a zero-energy basis composed solely of area-law states be constructed? States formed using Bethe ansatz methods usually exhibit low entanglement and are plausible candidates [67,68]. Second, do exact constructions beyond two-magnon states exist? So far, we see no immediate way to extend the character-theory-based fixed-separation method to a larger number of magnons. Most interesting would be the existence of nontrivial closed-form states in the largest symmetry sector, or with volume-law entanglement. Indeed, the presence of exponentially large null space may signify a hidden integrable structure, such as towers of states, possibly amendable to complementary analytical treatments. Finally, novel construction methods could be leveraged to build and stabilize zero-energy states, such as adaptive circuits [69,70], where repeated measurements may be utilized to project perturbed states back into the null-space manifold, mimicking the topological protection in surface codes, and making them valuable for fault-tolerant quantum computing.

Acknowledgments. A.P., B.M., and M.S. were funded by the European Research Council (ERC) under the European Union's Horizon 2020 research and innovation program (Grant Agreement No. 853368). C.J.T. was supported by an EPSRC fellowship (Grant Reference No. EP/W005743/1). The authors acknowledge the use of the UCL High Performance Computing Facilities (Myriad and Kathleen), and associated support services, in the completion of this work. M.S. was also supported by the Engineering and Physical Sciences Research Council (EPSRC) grant on Robust and Reliable Quantum Computing (RoaRQ), Investigation 004 (Grant Reference No. EP/W032635/1), and the EPSRC grant on (De)constructing Quantum Software (DeQS) (Grant Reference No. EP/Z002230/1). B.M. was also funded by DST, Government of India via the INSPIRE Faculty program. R.M. and H.J.C. acknowledge funding from National Science Foundation Grant No. DMR 2046570 and the National High Magnetic Field Laboratory. The National High Magnetic Field Laboratory is supported by the National Science Foundation through Grants No. NSF/DMR-1644779 and No. DMR-2128556 and the state of Florida.

DATA AVAILABILITY

The data that support the findings of this article are openly available [71].

[1] J. M. Deutsch, Quantum statistical mechanics in a closed system, Phys. Rev. A **43**, 2046 (1991).

[2] M. Srednicki, Chaos and quantum thermalization, Phys. Rev. E **50**, 888 (1994).

[3] L. D'Alessio, Y. Kafri, A. Polkovnikov, and M. Rigol, From quantum chaos and eigenstate thermalization to statistical mechanics and thermodynamics, Adv. Phys. **65**, 239 (2016).

[4] F. Borgonovi, F. M. Izrailev, L. F. Santos, and V. G. Zelevinsky, Quantum chaos and thermalization in isolated systems of interacting particles, Phys. Rep. **626**, 1 (2016).

[5] R. V. Jensen and R. Shankar, Statistical behavior in deterministic quantum systems with few degrees of freedom, Phys. Rev. Lett. **54**, 1879 (1985).

[6] M. Rigol and M. Srednicki, Alternatives to eigenstate thermalization, Phys. Rev. Lett. **108**, 110601 (2012).

[7] M. Rigol, V. Dunjko, and M. Olshanii, Thermalization and its mechanism for generic isolated quantum systems, Nature (London) **452**, 854 (2008).

[8] H. Kim, T. N. Ikeda, and D. A. Huse, Testing whether all eigenstates obey the eigenstate thermalization hypothesis, Phys. Rev. E **90**, 052105 (2014).

[9] W. Beugeling, R. Moessner, and M. Haque, Finite-size scaling of eigenstate thermalization, Phys. Rev. E **89**, 042112 (2014).

[10] N. Shiraishi, Proof of the absence of local conserved quantities in the *XYZ* chain with a magnetic field, Europhys. Lett. **128**, 17002 (2019).

[11] Y. Chiba, Proof of absence of local conserved quantities in the mixed-field Ising chain, Phys. Rev. B **109**, 035123 (2024).

[12] N. Shiraishi, Absence of local conserved quantity in the Heisenberg model with next-nearest-neighbor interaction, J. Stat. Phys. **191**, 114 (2024).

[13] H. K. Park and S. Lee, Proof of nonintegrability of the spin-1 bilinear-biquadratic chain model, Phys. Rev. B **111**, 134444 (2025).

[14] S. Moudgalya, S. Rachel, B. A. Bernevig, and N. Regnault, Exact excited states of nonintegrable models, Phys. Rev. B **98**, 235155 (2018).

[15] S. Moudgalya, N. Regnault, and B. A. Bernevig, Entanglement of exact excited states of Affleck-Kennedy-Lieb-Tasaki models: Exact results, many-body scars, and violation of the strong eigenstate thermalization hypothesis, Phys. Rev. B **98**, 235156 (2018).

[16] C. J. Turner, A. A. Michailidis, D. A. Abanin, M. Serbyn, and Z. Papić, Weak ergodicity breaking from quantum many-body scars, Nat. Phys. **14**, 745 (2018).

[17] C. J. Turner, A. A. Michailidis, D. A. Abanin, M. Serbyn, and Z. Papić, Quantum scarred eigenstates in a Rydberg atom chain: Entanglement, breakdown of thermalization, and stability to perturbations, Phys. Rev. B **98**, 155134 (2018).

[18] C.-J. Lin and O. I. Motrunich, Exact quantum many-body scar states in the Rydberg-blockaded atom chain, Phys. Rev. Lett. **122**, 173401 (2019).

[19] M. Schecter and T. Iadecola, Weak ergodicity breaking and quantum many-body scars in spin-1 XY magnets, Phys. Rev. Lett. **123**, 147201 (2019).

[20] S. Choi, C. J. Turner, H. Pichler, W. W. Ho, A. A. Michailidis, Z. Papić, M. Serbyn, M. D. Lukin, and D. A. Abanin, Emergent SU(2) dynamics and perfect quantum many-body scars, Phys. Rev. Lett. **122**, 220603 (2019).

[21] T. Iadecola and M. Schecter, Quantum many-body scar states with emergent kinetic constraints and finite-entanglement revivals, Phys. Rev. B **101**, 024306 (2020).

[22] K. Lee, R. Melendrez, A. Pal, and H. J. Changlani, Exact three-colored quantum scars from geometric frustration, Phys. Rev. B **101**, 241111(R) (2020).

[23] C. M. Langlett, Z.-C. Yang, J. Wildeboer, A. V. Gorshkov, T. Iadecola, and S. Xu, Rainbow scars: From area to volume law, Phys. Rev. B **105**, L060301 (2022).

[24] J. Wildeboer, C. M. Langlett, Z.-C. Yang, A. V. Gorshkov, T. Iadecola, and S. Xu, Quantum many-body scars from Einstein-Podolsky-Rosen states in bilayer systems, Phys. Rev. B **106**, 205142 (2022).

[25] A. N. Ivanov and O. I. Motrunich, Volume-entangled exact eigenstates in the PXP and related models in any dimension, Phys. Rev. Lett. **134**, 050403 (2025).

[26] Y. Chiba and Y. Yoneta, Exact thermal eigenstates of nonintegrable spin chains at infinite temperature, Phys. Rev. Lett. **133**, 170404 (2024).

[27] M. Serbyn, D. A. Abanin, and Z. Papić, Quantum many-body scars and weak breaking of ergodicity, Nat. Phys. **17**, 675 (2021).

[28] D. Bluvstein, A. Omran, H. Levine, A. Keesling, G. Semeghini, S. Ebadi, T. T. Wang, A. A. Michailidis, N. Maskara, W. W. Ho, *et al.*, Controlling quantum many-body dynamics in driven Rydberg atom arrays, Science **371**, 1355 (2021).

[29] A. Morvan, T. I. Andersen, X. Mi, C. Neill, A. Petukhov, K. Kechedzhi, D. A. Abanin, A. Michailidis, R. Acharya, F. Arute, *et al.*, Formation of robust bound states of interacting microwave photons, Nature (London) **612**, 240 (2022).

[30] E. J. Gustafson, A. C. Y. Li, A. Khan, J. Kim, D. M. Kurkcuoglu, M. S. Alam, P. P. Orth, A. Rahmani, and T. Iadecola, Preparing quantum many-body scar states on quantum computers, Quantum **7**, 1171 (2023).

[31] H. J. Changlani, D. Kochkov, K. Kumar, B. K. Clark, and E. Fradkin, Macroscopically degenerate exactly solvable point in the spin-1/2 kagome quantum antiferromagnet, Phys. Rev. Lett. **120**, 117202 (2018).

[32] J. Villain, R. Bidaux, J.-P. Carton, and R. Conte, Order as an effect of disorder, J. Phys. France **41**, 1263 (1980).

[33] E. F. Shender, Antiferromagnetic garnets with fluctuationally interacting sublattices, J. Exp. Theor. Phys. **56**, 178 (1982).

[34] C. L. Henley, Ordering due to disorder in a frustrated vector antiferromagnet, Phys. Rev. Lett. **62**, 2056 (1989).

[35] A. G. Green, G. Conduit, and F. Krüger, Quantum order-by-disorder in strongly correlated metals, Annu. Rev. Condens. Matter Phys. **9**, 59 (2018).

[36] A. Yu. Kitaev, Fault-tolerant quantum computation by anyons, Ann. Phys. (NY) **303**, 2 (2003).

[37] C. Nayak, S. H. Simon, A. Stern, M. Freedman, and S. Das Sarma, Non-abelian anyons and topological quantum computation, Rev. Mod. Phys. **80**, 1083 (2008).

[38] X. Chen, Z.-C. Gu, and X.-G. Wen, Local unitary transformation, long-range quantum entanglement, wave function renormalization, and topological order, Phys. Rev. B **82**, 155138 (2010).

[39] A. Y. Kitaev, Unpaired Majorana fermions in quantum wires, Phys. Usp. **44**, 131 (2001).

[40] D. A. Ivanov, Non-Abelian statistics of half-quantum vortices in p-wave superconductors, Phys. Rev. Lett. **86**, 268 (2001).

[41] V. Karle, M. Serbyn, and A. A. Michailidis, Area-law entangled eigenstates from nullspaces of local Hamiltonians, Phys. Rev. Lett. **127**, 060602 (2021).

[42] F. M. Surace, M. Votto, E. G. Lazo, A. Silva, M. Dalmonte, and G. Giudici, Exact many-body scars and their stability in constrained quantum chains, Phys. Rev. B **103**, 104302 (2021).

[43] D. Banerjee and A. Sen, Quantum scars from zero modes in an Abelian lattice gauge theory on ladders, Phys. Rev. Lett. **126**, 220601 (2021).

[44] S. Biswas, D. Banerjee, and A. Sen, Scars from protected zero modes and beyond in $U(1)$ quantum link and quantum dimer models, SciPost Phys. **12**, 148 (2022).

[45] I. Sau, P. Stornati, D. Banerjee, and A. Sen, Sublattice scars and beyond in two-dimensional $U(1)$ quantum link lattice gauge theories, Phys. Rev. D **109**, 034519 (2024).

[46] A. Udupa, S. Sur, S. Nandy, A. Sen, and D. Sen, Weak universality, quantum many-body scars, and anomalous infinite-temperature autocorrelations in a one-dimensional spin model with duality, Phys. Rev. B **108**, 214430 (2023).

[47] K. Hida, Crossover between the Haldane-gap phase and the dimer phase in the spin-1/2 alternating Heisenberg chain, Phys. Rev. B **45**, 2207 (1992).

[48] T. Kennedy and H. Tasaki, Hidden $Z_2 \times Z_2$ symmetry breaking in Haldane-gap antiferromagnets, Phys. Rev. B **45**, 304 (1992).

[49] K. Hida, Ground-state phase diagram of the spin-1/2 ferromagnetic-antiferromagnetic alternating Heisenberg chain with anisotropy, Phys. Rev. B **46**, 8268 (1992).

[50] H. Manaka, I. Yamada, and K. Yamaguchi, Ferromagnetic-dominant alternating Heisenberg chains with ferromagnetic and antiferromagnetic interactions formed in $(CH_3)_2CHNH_3CuCl_3$, J. Phys. Soc. Jpn. **66**, 564 (1997).

[51] H. Manaka and I. Yamada, Formation of alternating antiferromagnetic Heisenberg chains in $(CH_3)_2CHNH_3CuBr_3$, J. Phys. Soc. Jpn. **66**, 1908 (1997).

[52] M. P. Grabowski and P. Mathieu, Integrability test for spin chains, J. Phys. A: Math. Gen. **28**, 4777 (1995).

[53] B. Mukherjee, R. Melendrez, M. Szyniszewski, H. J. Changlani, and A. Pal, Emergent strong zero mode through local Floquet engineering, Phys. Rev. B **109**, 064303 (2024).

[54] A. W. Sandvik, Computational studies of quantum spin systems, AIP Conf. Proc. **1297**, 135 (2010).

[55] V. Oganesyan and D. A. Huse, Localization of interacting fermions at high temperature, Phys. Rev. B **75**, 155111 (2007).

[56] Y. Y. Atas, E. Bogomolny, O. Giraud, and G. Roux, Distribution of the ratio of consecutive level spacings in random matrix ensembles, Phys. Rev. Lett. **110**, 084101 (2013).

[57] B. Sutherland, Localization of electronic wave functions due to local topology, Phys. Rev. B **34**, 5208 (1986).

[58] M. Hamermesh, *Group Theory and Its Application to Physical Problems* (Dover Publications, Inc., Mineola, NY, 2003)

[59] B. E. Sagan, *The Symmetric Group* (Springer, New York, NY, 2001).

[60] See Supplemental Material at http://link.aps.org/supplemental/10.1103/rsm1-hzc3 for more details about character theory, tables of zero-energy degeneracies, and discussion of extra zero-energy states (Appendix A), detailed estimation of the exponential behavior (Appendix B), and detailed calculations of the von Neumann entanglement entropy of fixed-separation states (Appendix C).

[61] D. Husemöller, *Fibre Bundles*, 3rd ed. (Springer, New York, NY, 1994).

[62] L.-M. Duan, E. Demler, and M. D. Lukin, Controlling spin exchange interactions of ultracold atoms in optical lattices, Phys. Rev. Lett. **91**, 090402 (2003).

[63] F. Schäfer, T. Fukuhara, S. Sugawa, Y. Takasu, and Y. Takahashi, Tools for quantum simulation with ultracold atoms in optical lattices, Nat. Rev. Phys. **2**, 411 (2020).

[64] L.-K. Lim, A. Hemmerich, and C. M. Smith, Artificial staggered magnetic field for ultracold atoms in optical lattices, Phys. Rev. A **81**, 023404 (2010).

[65] H. Weimer, M. Müller, I. Lesanovsky, P. Zoller, and H. P. Büchler, A Rydberg quantum simulator, Nat. Phys. **6**, 382 (2010).

[66] H. Bernien, S. Schwartz, A. Keesling, H. Levine, A. Omran, H. Pichler, S. Choi, A. S. Zibrov, M. Endres, M. Greiner, *et al.*, Probing many-body dynamics on a 51-atom quantum simulator, Nature (London) **551**, 579 (2017).

[67] P. N. Bibikov, Bethe ansatz for two-magnon scattering states in 2D and 3D Heisenberg-Ising ferromagnets, J. Stat. Mech. (2018) 043108.

[68] Z. Zhang and G. Mussardo, Hidden Bethe states in a partially integrable model, Phys. Rev. B **106**, 134420 (2022).

[69] V. Ravindranath, Y. Han, Z.-C. Yang, and X. Chen, Entanglement steering in adaptive circuits with feedback, Phys. Rev. B **108**, L041103 (2023).

[70] A. J. Friedman, O. Hart, and R. Nandkishore, Measurement-induced phases of matter require feedback, PRX Quantum **4**, 040309 (2023).

[71] C. J. Turner, M. Szyniszewski, B. Mukherjee, R. Melendrez, H. J. Changlani, and A. Pal, Research data for “Stable infinite-temperature eigenstates in SU(2)-symmetric nonintegrable models”, University of Oxford’s Sustainable Digital Scholarship, Dataset, Figshare, 2026, https://doi.org/10.25446/oxford.32133277.